INSTITUTE OF PHYSICS PUBLISHING NANOTECHNOLOGY

Nanotechnology **12** (2001) 485–490 PII: S0957-4484(01)26780-4

Electrostatic force microscopy: principles and some applications to semiconductors

Paul Girard

Laboratoire d'Analyse des Interfaces et de Nanophysique (UMR CNRS 5011), Université de Montpellier II, Place E. Bataillon, 34095 Montpellier Cedex, France

E-mail: girard@lain.univ-montp2.fr

Received 7 July 2001, in final form 24 October 2001
Published 27 November 2001
Online at stacks.iop.org/Nano/12/485

Abstract
The current state of the art of electrostatic force microscopy (EFM) is presented. The principles of EFM operation and the interpretation of the obtained local voltage and capacitance data are discussed. In order to show the capabilities of the EFM method, typical results for semiconducting nanostructures and lasers are presented and discussed. Improvements to EFM and complementary electrical methods using scanning microscopy demonstrate the continuing interest in electrical probing at the nanoscale range.

(Some figures in this article are in colour only in the electronic version)

1. Introduction

Scanning force microscopy (SFM) has seen many developments in recent years [1], particularly in the detection of long-range forces such as magnetic [2] and electrostatic forces, including detection of charges [3–5] or voltages from low [6] and high frequencies [7, 8]. It is of technological interest to know the dc voltages and charges in semiconductor materials and structures, and electrostatic force microscopy (EFM) is the method used for their investigation.

In this paper we first describe the general principles of EFM, its expected performance with regard to spatial and voltage resolution, and the implementation of EFM as an addition to the atomic force microscope (AFM). Secondly, as observed on EFM imaging, the different levels of contrast are illustrated and applications of dc measurements to semiconductors are shown. Applications are made on material where normally existing surface voltages can be detected, and structures where, in addition, the effects of external applied voltage can be analysed. The properties of some complementary electrical SFM-like methods and some possible future EFM-like developments are discussed for low-dimensional devices.

2. Principles

Since EFM is mainly devoted to voltage detection and can lead to measurements of the local dc voltage, we shall essentially concentrate on this point.

When a voltage V occurs between a sample and the EFM sensor maintained at close proximity, the electrostatic force F can be written as:

$$F = \tfrac{1}{2}\mathrm{d}C/\mathrm{d}z\, V^2 \qquad (1)$$

where C is the tip to sample capacitance.

We assume that the voltage V is composed of the contact potential V_{cp} plus applied dc and sinusoidal voltages, V_{dc} and V_{ac} respectively, with, in addition, an externally induced surface voltage $V_{induced}$ related to the extra dc voltages on an operating device, for example $V = (V_{cp} + V_{dc} + V_{induced}) + V_{ac} \sin \Omega t$.

Then, referring to the frequency, i.e. dc, Ω or 2Ω, the force can be decomposed into three terms. Firstly

$$F_{dc} = \tfrac{1}{2}\mathrm{d}C/\mathrm{d}z[(V_{dc} + V_{cp} + V_{induced})^2 + \tfrac{1}{2}V_{ac}^2] \qquad (2)$$

which bends the cantilever continuously but which is difficult to detect. Secondly

$$F_{\Omega} = \mathrm{d}C/\mathrm{d}z(V_{dc} + V_{cp} + V_{induced})V_{ac} \sin \Omega t. \qquad (3)$$

This term has a simple linear dependence on the capacitive coupling $\mathrm{d}C/\mathrm{d}z$ and the sample voltages V_{cp} and $V_{induced}$. So capacitive coupling and voltage contrasts are expected to be seen on the force signal F_{Ω}. Using signal processing it can easily be extracted from noise and imaged when scanning the sample at a constant tip–sample distance.

 © 2001 IOP Publishing Ltd Printed in the UK

If, in addition, a closed loop injects a voltage V_{dcK} such as $F_{\Omega} = 0$, i.e. $V_{dcK} = -(V_{cp} + V_{induced})$, surface voltage variations related either to V_{cp} or to $V_{induced}$ can be measured and imaged; this is called nano-Kelvin operation. The third term

$$F_{2\Omega} = -\tfrac{1}{4}\mathrm{d}C/\mathrm{d}z V_{ac}^2 \cos 2\Omega t \qquad (4)$$

depends on local capacitive coupling.

If only ac signals are involved, with different frequencies on the tip and the sample, the V^2 behaviour is mixed, giving rise to bending of the cantilever at both the sum and the difference of frequencies. So, even in the gigahertz range the presence of a voltage on the sample can be analysed [7, 8] if the frequency difference is in the kilohertz range.

If charges are involved instead of voltages, an F_{Ω} signal is also observed [4, 9]. It is generally assumed that an insulator, bringing charges to its surface at a distance z from the tip, is sandwiched between a conducting plane and the EFM sensor, and that voltages are applied similarly to the case we examined first. Then a supplementary Coulomb force arises between the static charge Q_s of the sample and the ac charge induced on the tip, i.e. CV_{ac}. Then F_{Ω} can be written as

$$F_{\Omega} = [\mathrm{d}C/\mathrm{d}z(V_{cp} + V_{dc}) - Q_s C/(4\pi\varepsilon_0 z^2)]V_{ac} \sin \Omega t. \quad (5)$$

So the sign and position of charges Q_s can be obtained, but their measurement strongly depends on the particular tip to sample configuration and is not as simple as for voltages.

Thus by using the EFM non-contact method physical data such as surface to bulk sample capacitance and dc surface voltages can be measured. The localization of dc charges and high-frequency voltages has been reported. However, the scale of performance has to be precise in terms of voltage resolution but also in terms of spatial resolution if application to the analysis of low-dimensional semiconductor devices is to happen.

3. Expected performances

3.1. Sensor configuration

Since the sensor is composed of a cantilever which holds a conical tip ending at a spherical apex of radius R (in the range 30–50 nm), the total sensor–plane (both assumed to be conducting) sample capacitor is effectively composed of three capacitors in parallel (cantilever, cone and apex) [10].

So the force can be written as

$$F = \tfrac{1}{2}(\mathrm{d}C_{cantilever}/\mathrm{d}z + \mathrm{d}C_{cone}/\mathrm{d}z + \mathrm{d}C_{apex}/\mathrm{d}z)V^2. \qquad (6)$$

In figure 1, the numerical calculations of force versus distance show successively the effect of the apex, cone and cantilever, in accordance with experiments. The best conditions of resolution for the cantilever structure have been established: a tip height as long as possible and a half-cone angle θ as low as possible plus a slight 20° cantilever tilt [11]. The use of the force gradient improves localization of the electrostatic interaction on the part of the sensor near the sample and also localizes the area of interaction on the sample.

Naturally, the best case is obtained when only the tip to apex interaction is involved, i.e. $z < R/2$. Then, if the apex corresponds to a sphere of radius R placed at a distance z from

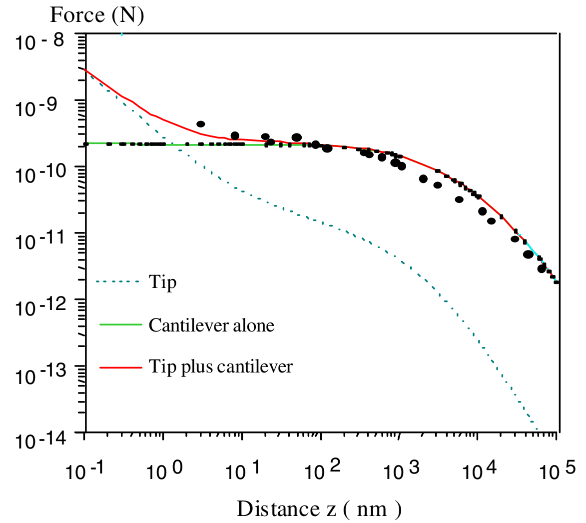

Figure 1. Force versus distance for 1 V applied. Experimental results (dots) correspond to a typical EFM sensor (cantilever 100 μm long with 10° tilt, tip height 4 μm, $R = 10$ nm). The force related to the cantilever remains constant until its initial distance to the sample is appreciably changed. The force of the tip alone (dots) shows first a linear (apex interaction) then a supralinear (cone interaction) and finally a quadratic behaviour versus the tip to sample distance. The tip plus cantilever force (continuous curve) is more complex, since the presence of the cantilever disturbs the field lines, and the apex regime is limited to small distances.

a conducting plane of infinite dimensions, the force can be written as

$$F = \pi\varepsilon_0(R/z)V^2. \qquad (7)$$

The tip to sample distance z, the apex radius R and their stability are the key points for the experiments. A compromise has to be found for the radius: the smaller the radius, in principle the better the resolution becomes, but then the influence of the cone and cantilever may increase [12].

3.2. Resolution

The spatial resolution for an electrical force has been calculated when the tip explores, at a constant distance, a 0–1 V voltage step in a plane, the tip being at 0 V. In this case the force is zero on one side of the step and maximum on the other side. The resolution is estimated as the length of the transition from 25 to 75% of the maximum force [13]. For apex distances z greater than 3 nm, the resolution Res is proportional to z, i.e. Res $= 5z$, so 50 nm is expected for $z = 10$ nm, which corresponds to recently reported data [14]. For distances less than 3 nm, the electrical field is practically perpendicular to the end of the apex, and then Res $\cong 2(2/3Rz)^{1/2}$, so the nanometre range is attained at nanometre distances. For charges close to the surface of an insulator, the simulation gives a resolution not too far from $R + z$.

If the detected voltage is limited by the thermal noise, the voltage resolution can be written as [15]

$$V_{cp\,min} = (2k_B T k B/\pi^3 Q f_{res})^{1/2}(1/\varepsilon_0 V_{ac})(z/R). \qquad (8)$$

Using $f_{res} = 75$ kHz, $k = 3$ N m^{-1}, $Q = 200$, $R = 50$ nm, $z = 10$ nm, $V_{ac} = 0.5$ V, $B = 300$ Hz, then $V_{cp\,min} = 5$ mV which is sufficient for many applications.

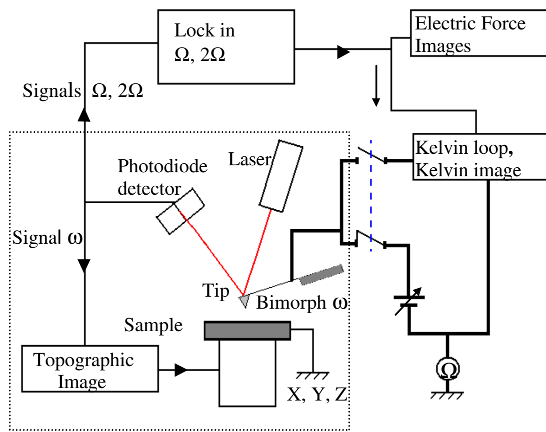

Figure 2. Schematic diagram of the electrostatic force microscope generally based on a commercial AFM (inside dotted box). Two lock-ins allow the detection of the Ω and 2Ω signals and a closed loop brings the surface voltage.

4. Using an EFM for dc measurements

In order to keep the tip to sample distance z constant and to obtain the morphology of the sample the sensor is usually mechanically driven near the resonance frequency and the atomic force microscopy (AFM) loop maintains the vibration amplitude constant and equal to z [16] when scanning. The EFM method is generally based on the following assumption: the electrostatic forces act as a second-order effect on the mechanical oscillation; this can occur when a similar topographic image is obtained in both contact and vibrating modes. Detection of the bending of the cantilever at Ω and 2Ω, in many cases at frequencies much lower than the resonance, is obtained via external lock-in amplifiers and gives the electrical forces. To achieve nano-Kelvin operation, a supplementary loop allows a counter voltage to be injected on the tip in order to obtain the image of the surface voltage (equation 3, figure 2). Since these measurements require a stable, constant tip to sample distance we have to briefly recall the two ways to obtain this.

4.1. Single-pass method

In ambient oscillating operation, the mechanical amplitude of oscillation near the resonance is usually weakly dependent on the electrostatic force gradient. Then, under low dc voltages, the topography is obtained simultaneously to $F_{2\Omega}$ and F_{Ω} for nano-Kelvin operation [17, 18]. However, if high V_{cp} or V_{dc} occur, the force gradient can influence the mechanical amplitude and the sharpness of the topographic image is degraded. Consequently, when V_{cp} is suppressed using nano-Kelvin operation, the image quality is restored.

Under a vacuum [19, 20], since the quality coefficient of the resonance is strongly improved, amplitude regulation is no longer feasible and the topography is obtained by keeping the frequency shift $\Delta f/f$ constant. This can be generally written, assuming a low oscillation amplitude, as

$$\Delta f/f = \tfrac{1}{2}\text{Grad } F_z/k. \quad (9)$$

Since electrostatic force gradients Grad F_z are always present, the topography is expected to be dependent on local voltages and charges, and the effect of nano-Kelvin operation on topography is probably more important.

4.2. Double-pass method, line by line operation

A first scan of a line allows acquisition of the morphology, generally obtained in the 'tapping' mode. Using a second pass on the same line, with an additional retraction (some tens of nanometres) from the sample (or 'lift'), the sensor is driven into oscillation at the resonance frequency either by the electrical signal on which Kelvin operation is based or mechanically. In the latter case, since the cantilever oscillates freely with a reasonable quality coefficient of resonance, the phaseshifts induced by the force gradients can be detected [21]. The drawback is certainly some reduction in resolution due to the increase in the tip to sample distance in comparison with the single-pass method.

5. Interpretation and application to semiconductors

5.1. Detection of normally existing surface voltages

The first idea was to image inhomogeneities of work function on metals, an application which proved the validity of the nano-Kelvin concept [22]. Other authors have used nano-Kelvin operation to characterize the presence of local doping [23]. For example this method could be extended to test electron emitting tips such as those used as sources in scanning electron microscopy (SEM). On nanostructures such as InAs nanoislands grown on GaAs Kelvin voltage changes have been shown with resolutions better than 20 mV and 20 nm [24]. Simple force imaging, i.e. F_{Ω}, has demonstrated the inhomogeneities on GaN thin films which have been correlated with electron transport properties [25].

On F_{Ω}, the capacitive coupling contrast, already seen on other structures [24], has been clearly established (figure 3). The experimental test is the inversion of contrast when changing the effective dc voltage that causes phase reversal of F_{Ω} (equation 3). There are two reasons for this decrease of $\mathrm{d}C/\mathrm{d}z$ when meeting a local bump: the sensor is retracted from the sample surface and the capacitance of the tip apex changes from that of a sphere plane to that of a sphere (i.e. the top of the bump). So whether the whole sensor or only the apex is involved in capacitive coupling, there is always a reduction in $\mathrm{d}C/\mathrm{d}z$. Conversely, when meeting a 'dip', $\mathrm{d}C/\mathrm{d}z$ increases. The surface topography is therefore the origin of the capacitive coupling contrast that could mask voltage variations by force observations. Variations in $\mathrm{d}C/\mathrm{d}z$ can be easily detected with $F_{2\Omega}$ too.

For a semiconductor laser structure [18], four types of information have been obtained simultaneously, i.e. morphology, capacitive coupling and surface (or Kelvin) voltage amplitudes, plus their spatial distributions (figure 4). On the cleaved surface, since these parts are richer in aluminium, there is preferential oxidation which produces topographic variation thus aiding electrical observations. Here, a local decrease in capacitive coupling could be related to the presence of areas of junction depletion underneath the surface. This supplementary capacitor arises in series with the capacitance of the tip to surface air gap and gives a second source for capacitive coupling contrast. The changes in

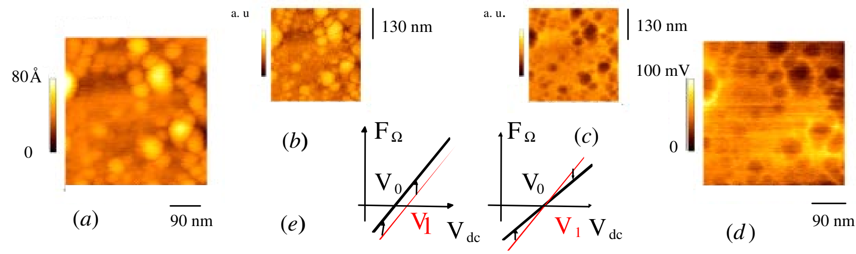

Figure 3. Observation of InAs/GaAs nanoislands on a 400 × 400 nm^2 scale: (*a*) morphology, (*b*) and (*c*) F_Ω for a dc voltage of + and −2 V respectively, (*d*) nano-Kelvin voltage distributions. The inversion of F_Ω contrast with the sign of V_{dc} is related to the slopes of dC/dz on the plane and on the bump areas, as seen on graph (*e*). If only voltage differences are present, no contrast inversion occurs.

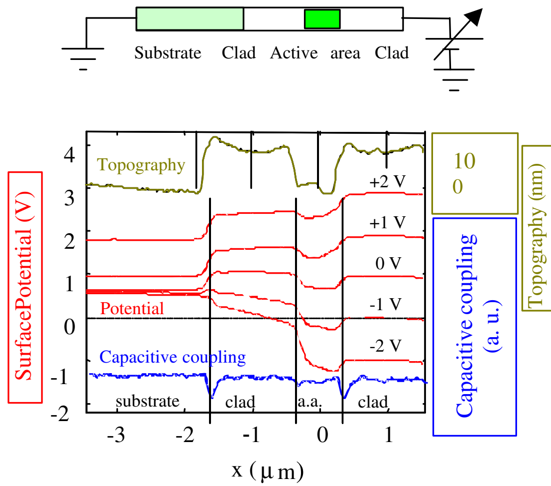

Figure 4. Example of observations on a laser structure: the upper part shows the structure and the lower part the EFM observations. The topography, voltage measurements (under different polarizations as indicated) and capacitive coupling are reported (from top to bottom) and simultaneously observed.

surface contact potential would certainly be more significant if observed in ultra-high vacuum on cleavages [26], but the values of the observed voltage shifts are a good indication of contact potentials too, and have the simplicity of air observations [27]. The surface potential is rich in information since it can be related to the nature and crystalline orientation of the material, the presence of surface states and different dopings.

The spatial extents of force, capacitive coupling and Kelvin voltage are related to the doping or semiconductor dimensions, so these data may be useful for quality control of the technology.

5.2. Detection of externally induced surface voltages

Reports about internal potential measurements on operating devices have appeared in the literature for silicon pn junctions [28], resistors [29], nipi [30], light emitting [17] and laser [18] structures.

On an operating semiconductor laser structure, the voltage distribution can easily be deduced from figure 4 under different external polarizations, so non-contact nanopotentiometry is achievable. This opens the way for device optimization, for example in terms of power distribution along the structure, and in the near future to computer-assisted device design if all the voltage distributions are known, including inside the lowest-dimensional parts.

Cleavage of silicon devices [31] opens the way to failure analysis and the control of the technological process; due to the requirements of industry the preparation of working cross sections with mechanical polishing is now becoming routine [32].

5.3. Other electrical methods

Supplementary electrical characterization methods have recently been used in connection with voltage contrast analysis deduced from the now widely used SEM [33]. They are based on measurements where the tip remains in contact with the sample. First we could mention contact nanopotentiometry, i.e. the voltage difference between a scanning tip and a reference point on the sample, which shows resolutions of some tens of nanometres [30, 34]. In addition, the point contact resistance at the semiconductor–tip interface is a way to localize differently doped areas [35], while the spreading resistance, once calibrated, leads to knowledge of the level of local doping [36]. Measuring the scanning capacitance, or nano-$C(V)$ [37], is the ultimate aim, since it allows a nice spatial resolution and, after calibration, is connected to the level of doping [38]. Simply using the capacitance C, suitable spatial resolution is due to the fact that only voltage-dependent capacitances are taken into account, and these changes come from the area of interest, i.e. the semiconductor underneath the tip.

6. The near future

6.1. Improvement of EFM performance: electrostatic force gradient microscopy

With force gradient detection it is hoped to image localized charges or charged areas [4, 39, 40] and semiconductor doped zones [41], especially in dc regimes. In comparison with force measurements, interest in force gradient detection resides in a better localization of the electrostatic interaction [10, 11]. It has recently been proposed that force gradients at different frequencies (see section 2) be used to image voltages and capacitive couplings and to measure voltages [21]. An increased significance of the measurements has been shown, especially when the tip to sample distance increases as in the double-pass method (figure 5), and, *a fortiori*, at close proximity.

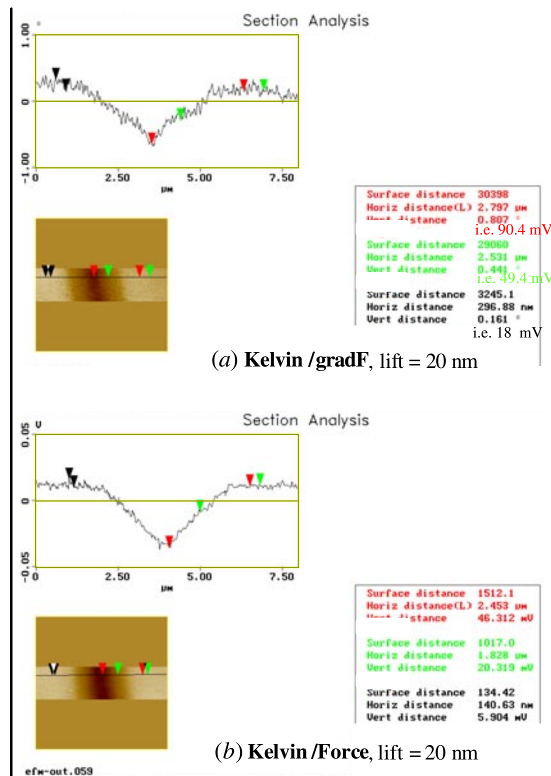

(*a*) **Kelvin /gradF**, lift = 20 nm

(*b*) **Kelvin /Force**, lift = 20 nm

Figure 5. Comparison of voltage measurements using (*a*) the Kelvin force gradient and (*b*) Kelvin force measurements on a sawtooth like voltage shape. An improvement in sharpness is clearly seen using the gradient instead of force and there is a significant voltage difference on the centre and sides of the voltage accident. Since the force gradient measurement area is more localized than the force measurement area, a more realistic value is observed.

6.2. Extension to other conditions and other SFM

Vacuum or low-temperature AFM and EFM methods have been reported [20, 42–45] and these methods are becoming fully developed. Active sensors, and consequently multisensor AFMs, are under study [46] and they could be extended from ambient to the more constraining experimental conditions required for fundamental studies. We can imagine them having the capability to inject currents and detect voltages on the nanocontact scale.

7. Conclusions

Based on AFM equipment, EFM is now an experimentally established method for local observations and measurements on semiconductors. In addition to morphology, three other classes of data related to electrical characterization can be obtained: nano-Kelvin operation gives the work function which can be correlated with surface to bulk capacitances; the spatial extent of constant voltages, force or capacitance, particularly for any low-dimensional semiconductor structure; the local voltage behaviour on an operating structure, or non-contact nanopotentiometry. All these data are important for technological process control and failure analysis.

Improvements in spatial resolution, as recently shown in electrostatic force gradient microscopy, make EFM of even greater interest in connection with other electrical methods such as scanning capacitance or spreading resistance. Finally, concerning more fundamental studies, the capability for nanoconnection with AFM-like methods could offer in the near future the ability to explore the electrical or optical behaviour of individual nanostructures.

Acknowledgments

I would like to particularly acknowledge colleagues from Montpellier University—G Leveque, S Belaidi, M Ramonda and Cl Alibert—and from the Ioffe Institute—A N Titkov, A N Usikov and W Lundin—who either participated in the work or provided samples.

References

[1] Binnig G, Gerber Ch, Stoll E, Albrecht T-R and Quate C-F 1987 *Europhys. Lett.* **3** 1281
[2] Martin Y and Wrickramasinghe H K 1987 *Appl. Phys. Lett.* **50** 1455
[3] Terris B D, Stern J E, Rugar D and Mamin H J 1989 *Phys. Rev. Lett.* **63** 2669
[4] Schonenberger C, Alvarado S F, Lambert S E and Sanders I L 1990 *J. Appl. Phys.* **67** 7278
[5] Saurenbach F and Terris B D 1990 *Appl. Phys. Lett.* **56** 1704
[6] Martin Y, Abraham D W and Wrickramasinghe H K 1988 *Appl. Phys. Lett.* **52** 1103
[7] Hou A S, Ho F and Bloom D-M 1988 *Electron. Lett.* **28** 203
[8] Bohm C, Saurenbach F, Taschner P, Roths C and Kubalek E 1996 *J. Phys. D: Appl. Phys.* **26** 842
[9] Nyffenegger R M, Penner R M and Schierle R 1997 *Appl. Phys. Lett.* **71** 1878
[10] Belaidi S, Girard P and Leveque G 1997 *J. Appl. Phys.* **81** 1023
[11] Belaidi S, Girard P and Leveque G 1997 *Microelectron. Reliab.* **37** 1627
[12] Jacobs H O, Leuchtmann P, Hoffman O J and Stemmer A 1997 *J. Appl. Phys.* **84** 1168
[13] Belaidi S, Lebon F, Girard P, Leveque G and Pagano S 1998 *Appl. Phys.* A **66** S239
[14] O'Boyle M P, Hwang T T and Wrickramasinghe H K 1999 *Appl. Phys. Lett.* **74** 2641
[15] Nonnenmacher M, O'Boyle M P and Wrickramasighe H K 1991 *Appl. Phys. Lett.* **58** 2921
[16] Burnham N A, Kulik A J, Gremaud G, Gallo P J and Ouveley F 1996 *J. Vac. Sci. Technol.* B **14** 794
[17] Shikler R, Meoded T, Fried N and Rosenwacks Y 1999 *Appl. Phys. Lett*. **74** 2972
[18] Leveque G, Girard P, Skouri E and Yareka D 2000 *Appl. Surf. Sci.* **157** 251
[19] Giessibl F J 1994 *Japan. J. Appl. Phys.* **33** 3726
[20] Sommerhalter Ch, Mattes Th W, Glatzel Th, Jäger-Waldau A and Lux-Steiner M Ch 1999 *Appl. Phys. Lett.* **75** 286
[21] Girard P and Ramonda M 2001 *Proc. SPM'01 (Vancouver, Canada)* NRC-CNRC 338
[22] Nonnenmacher M, O'Boyle M and Wrickramasinghe H K 1992 *Ultramicroscopy* **42–4** 268
[23] Henning A-K, Hochwitz T, Slinkman J, Never J, Hoffman S, Kaszuba P and Daghlian Ch 1995 *J. Appl. Phys.* **77** 1888
[24] Titkov A N, Girard P, Evtikhiev V P, Ramonda M, Tokranov V E and Ulin V P 1999 *NC-AFM 99 Conf. Abst. (Pontresina, Switzerland)* p 25
[25] Shmidt N M, Emtsev V V, Kryzhanovsky A S, Kyutt R N, Lundin V W, Poloskin D S, Ratnikov V V, Sakharov A V, Titkov A N, Usikov A S and Girard P 1999 *Phys. Status Solidi* b **216** 581
[26] Guasch C, Doukkali A and Bonnet J J 2001 *J. Vac. Sci. Technol.* A **19-5** 205
[27] Ankudinov A, Titkov A, Evtikhiev V, Kotelnikov E, Lvshiz D, Tarasov I, Egorov A, Riebert H, Huhtinen H and Laiho R 2001 *Conf. Proc. Nanostructures Symp. (Repino, Russia)*

[28] Kikukawa A, Hosada S and Imura R 1995 *Appl. Phys. Lett.* **66** 3150
[29] Vatel O and Tanimoto M 1995 *J. Appl. Phys.* **77** 2358
[30] Chavez-Pirson A, Vatel O, Tanimoto M, Ando H, Iwamura H and Kanbe H 1995 *Appl. Phys. Lett.* **67** 2358
[31] Nxumalo J N, Shimitzu T D and Thompson D J 1996 *J. Vac. Sci. Technol.* B **14** 386
[32] Trenkler T, Stephenson R, Jansen P and Vandervorst W 2000 *J. Vac. Sci. Technol.* B **18** 586
[33] Girard P 1992 *J. Physique* **6** 259
[34] Shafai C, Thomson D J and Simard-Normandin M 1994 *J. Vac. Sci. Technol.* B **12** 378
[35] Houze F, Meyer R, Schneegans O and Boyer L 1996 *Appl. Phys. Lett.* **69** 1975
[36] De Wolf P, Geva M, Hantschel T, Vandervorst W and Bylsma R B 1998 *Appl. Phys. Lett.* **75** 2155
[37] Sze S M 1981 *Physics of Semiconductor Devices* (New York: Wiley)
[38] Williams C C 1999 *Ann. Rev. Mater. Sci.* **29** 471
[39] Yokoyama H, Inoue T and Itoh J 1994 *Appl. Phys. Lett.* **65** 3143
[40] Jones J T, Bridger P-M, Marsh O J, Mc Gill T C 1999 *Appl. Phys. Lett*. **75** 1326
[41] Nelson M W, Scroeder P G, Schlaf R and Parkinson B 1999 *J. Vac. Sci. Technol.* B **17** 1364
[42] Allers W, Schwartz A, Schwartz U-D and Wiesendanger R 1998 *Rev. Sci. Instrum.* **69** 221
[43] Kikukawa A, Hosaka S and Imura R 1995 *Appl. Phys. Lett.* **66** 3510
[44] Gütner P 1996 *J. Vac. Sci. Technol.* B **14** 2428
[45] Kitamura S and Iwatsuki M 1998 *Appl. Phys. Lett.* **72** 3154
[46] Vettiger P, Despont M, Dreschler U, Dig U, Herle W, Lutwyche M I, Rothuizen H, Stutz R, Widmer R and Binnig G K 1999 *Proc. STM'99 Conf. (Seoul)* ed Y Kuk, I W Lyo, D Jeon and S I Park, p 4